

Second Order Differential Properties of Tensor Product Fractal Surfaces

Clement Poull^a, Christian Gentil^b, Celine Roudet^c, Lucie Druoton^d and Michaël Roy^e

Laboratoire d'Informatique de Bourgogne (LIB), University of Burgundy, 9 Av. Alain Savary, 21000 Dijon, France
{clement.poull, christian.gentil, celine.roudet, lucie.druoton, michael.roy}@u-bourgogne.fr

Keywords: Surface, Fractal Geometry, Iterated Function System (IFS), Nowhere Differentiability, Tangent, Curvature.

Abstract: Many domains require non-smooth surface geometries: industry with quality control or CAD, computer graphics with geometric texture generation or terrain synthesis... Fractal models like the Iterated Function Systems (IFS) model are capable of generating self-similar multiscale objects, allowing the generation of a large variety of surfaces with non-standard geometries. Preceding works on IFS have demonstrated how to compute and control pseudo-tangents (defined by two different directions for the right and left tangents at each point) everywhere on these nowhere differentiable geometries. The second-order differential form, that provides even more control possibilities, was only proposed for fractal curves via the introduction of the Differential Characteristic Function (DCF). In this paper, we introduce the Surface Differential Characteristic Function (SDCF), an analytical form that helps characterising and analysing the differential properties (tangents and curvatures) of tensor product non-differentiable surfaces. We use the SDCF to compute the pseudo-curvatures for surfaces generated by tensor products of IFS.

1 INTRODUCTION

For polynomial or rational models like Bézier, subdivision, or NURBS curves and surfaces, the computation of their derivatives is straightforward and known for a long time. When an application requires non-standard geometry, such as terrain generation or geometric texture synthesis, the need for more complex models arises. Such methods include procedural noises, geomorphologic simulations, or fractal-based methods. For the latter, the generated surfaces often present two characteristics: irregularity (non-differentiability) and self-similarity (similar geometry at all scales). Bolzano and Takagi (Bolzano, 1950; Takagi, 1901) recursively defined functions were likely designed with these two properties in mind. Analysing the differential properties of such surfaces is a novel approach as such surfaces were initially presented as non-differentiable, but differential properties still exist.

From a mathematical point of view, the irregularity of a function was also studied by introducing "fractional continuity" like the Hölder coefficient or

Kolwankar local fractional derivative. Bensoudane (Bensoudane et al., 2009) applies these methods to analyze rough curves generated by the FIF model. He proves that even if such fractal curves are nowhere differentiable, it is possible to define a right and a left tangent. The angle between the right and left tangent gives information on the roughness. Podkorytov (Podkorytov et al., 2014; Podkorytov et al., 2013) extends these results to P-IFS free-form curves and surfaces by proposing a definition of a pseudo-tangent hyperplane by an eigenanalysis of subdivision matrices. He applies this definition to create a connection between curves and rough surfaces.

All these studies deal with the first-order derivative for the deterministic procedural generation process. Some works focus on the second-order derivative to estimate the surface curvature. For data coming from an acquisition process or produced from a procedural stochastic process, the primary approach consists of computing a function approximating the data at a given scale level and computing the curvature from the function (Bigerelle et al., 2013). Then, many questions arise: How do we fit data? What is the appropriated scale level? What is the sensibility to the noise or random process?

Our work aims at providing a framework to analyse the differential properties of nowhere-differentiable surfaces, specifically fractal surfaces.

^a <https://orcid.org/0000-0002-4402-2928>

^b <https://orcid.org/0000-0002-0343-3456>

^c <https://orcid.org/0000-0002-0704-081X>

^d <https://orcid.org/0000-0002-6409-8516>

^e <https://orcid.org/0009-0002-4727-0334>

Various fractal models exist, including L-Systems by Lindenmayer (Lindenmayer, 1968) and Iterated Function Systems (IFS) by Hutchinson (Hutchinson, 1981), popularized by Barnsley with Fractal Interpolation Functions (FIF) (Barnsley, 1988; Barnsley, 1986). We focus on an extension to IFS: Projected IFS (P-IFS) defined by Zair (Zair and Tosan, 1996) due to their deterministic nature (thus allowing predictable reasoning about their differential properties), the control possibilities they offer thanks to their free-form deformations, and the large variety of forms they can generate, from subdivision surfaces to chaotic curves. We propose a theoretical study based on Janbein et al.'s Differential Characteristic Functions (Janbein et al., 2024) to compute the pseudo-curvature of tensor-product surfaces thanks to the Surface Differential Characteristic Function, that can be defined as a tensor product of DCF.

We start by providing background on IFS, P-IFS, tensor product surfaces, and the DCF needed for understanding the rest of this paper. Then we define the SDCF, and explore the first and second-order differential properties brought by this construct. Finally, we detail how to compute pseudo-curvature using this function, before concluding with potential applications and perspectives.

2 BACKGROUND

We introduce necessary notions for the study of pseudo-curvature of fractal models and their pseudo-curvature. Hence we first present the common model used for generating fractal shapes in a deterministic way through affine transformations (called Iterated Function System: IFS). We continue with the model we considered here (called Projected Iterated Function System: P-IFS) that also allows free form deformations thanks to control points. Then, we recall notions on tensor products and barycentric coordinate systems that we used to create fractal surfaces from fractal curves. Finally, we showcase the Differential Characteristic Function (DCF) (Janbein et al., 2024), a differential geometry approach used to analyze the IFS-generated curves. We conclude this section by highlighting some important results its authors obtained.

2.1 Iterated Function System

Introduced by Hutchinson in (Hutchinson, 1981) and popularized by Barnsley in (Barnsley, 1988), an Iterated Function System (IFS) is a finite set of contractive operators $\mathbb{T} = \{T_i : \mathbb{X} \mapsto \mathbb{X}\}_{i=0}^{I-1}$ where (\mathbb{X}, d) is

a complete metric space, typically \mathbb{X} is either \mathbb{R}^2 or \mathbb{R}^3 and d is the euclidean distance. The Hutchinson operator $\mathbb{T}(K)$ consists in applying all the operators T_i to K , an arbitrary non-empty subset of compacts of \mathbb{X} : $\mathbb{T}(K) = \bigcup_{i=0}^{I-1} T_i K$. As each operator is a contraction, the Hutchinson operator duplicates K in I smaller copies. Note that \mathbb{T} is also a contractive operator in (\mathbb{X}, D_h) where D_h is the Hausdorff distance associated to (\mathbb{X}, d) (Barnsley, 1988). Banach fixed-point theorem (Banach, 1922) states that there exists a unique non empty compact \mathcal{A} of \mathbb{X} such that it satisfies the self-similarity property: $\mathbb{T}(\mathcal{A}) = \mathcal{A}$. In other word, \mathcal{A} is constructed as an infinite union of smaller copies of itself. This fixed point \mathcal{A} is called the attractor of \mathbb{T} , as it is the limit of iteratively applying the Hutchinson operator to K : $\mathcal{A} = \lim_{n \rightarrow \infty} \mathbb{T}^n(K)$, while being independent of K . Note that the geometry of the attractor \mathcal{A} does not depend on the choice of K , but only on the operators of \mathbb{T} . This approach allows the modeling of a large family of self-similar objects.

We define a dyadic point as any point that can be expressed as a finite sequence of transformations.

2.2 Projected Iterated Function System

An extension of the IFS model was presented by Zair et al. (Zair and Tosan, 1996) as the Projected Iterated Function System (P-IFS), in order to allow free-form deformations of the attractor, akin to Bezier curves or NURBS.

If the attractor (and the associated operators) is defined in \mathbb{B}^N (called the barycentric space), a N -dimensional vector of control points $(P_i \in \mathbb{X})_{i=0}^{N-1}$ can be used to control the global geometry of the attractor. The same attractor defined in barycentric space can be projected to a different geometry in the projection space depending on the control points considered. This process is similar to the subdivision process used to construct Bezier curves in a barycentric space, followed by a projection according to the control points.

Notation and Working Hypotheses: In this paper, we only consider curve P-IFS with two operators that are linear contractive operators represented by matrices in a barycentric space. We use the same symbol to represent the operator or its matrix. We designate by λ_i the eigenvalues of such a matrix and \mathbf{v}_i its associated eigenvector. We index the eigenvalues in strictly decreasing order of modulus and require that they are all of distinct modulus. Since the operators are contractive, all the eigenvalues of the matrix are lesser than one, except one that is exactly 1. For this latter, its associated eigenvector is not a vector but a point

(its coordinates sum to 1 instead of 0 for the other eigenvectors) and corresponds to the fixed point of the operator. Bezier curves are a specific case of P-IFS where the attractor is the Bernstein polynomial basis functions, and the operators are the De Casteljaun matrices, as shown by Zair (Zair and Tosan, 1996).

Each attractor discussed in the following is composed of a set of points in \mathbb{B}^N , where each point is interpreted as a set of weights w.r.t. the control points. We note $P\mathcal{A}$ the projection of an attractor \mathcal{A} from the barycentric space to the modeling space: $P\mathcal{A} = \{P\omega; \omega \in \mathcal{A}\}$. $P\omega$ represents the projection of any set of weights ω w.r.t. the control points P : $P\omega = \sum_{i=0}^{N-1} P_i \omega_i$ where ω_i is the i^{th} element of ω .

2.3 Tensor Product and IFS

In this study, we focus on fractal surfaces defined from the tensor product of fractal curves, in the same manner as Bezier surfaces can be constructed from Bezier curves. In the case of P-IFS, this corresponds to the pair-wise tensor product of the cartesian product of two P-IFS as shown by Zair (Zair, 1998).

Given two P-IFS $\mathbb{T} = \{T_i : \mathbb{B}^N \mapsto \mathbb{B}^N\}_{i=0}^{I-1}$ and $\mathbb{T}' = \{T'_j : \mathbb{B}^M \mapsto \mathbb{B}^M\}_{j=0}^{J-1}$, their tensor product is: $\mathbb{T}^\otimes = \{T_{ij} : \mathbb{B}^{NM} \mapsto \mathbb{B}^{NM}\}_{i=0, j=0}^{I-1, J-1}$ where $T_{ij} = T_i \otimes T'_j$.

The attractor \mathcal{A} of this new P-IFS \mathbb{T}^\otimes is the tensor product of the attractors of \mathbb{T} and \mathbb{T}' , resulting in a surface once it is projected into the modeling space by a set of NM control points. An example of such a surface is illustrated by Figure 1 as the tensor product of a Takagi curve and a Bezier curve.

Notation: In the following, we focus on the behavior of the convergence of a single operator. Hence we use $\mathcal{T} = T \otimes T'$ with $T : \mathbb{B}^N \mapsto \mathbb{B}^N$, $T' : \mathbb{B}^M \mapsto \mathbb{B}^M$ and $\mathcal{T} : \mathbb{B}^{NM} \mapsto \mathbb{B}^{NM}$. We designate by Λ_k the eigenvalues of \mathcal{T} and \mathbf{V}_k its associated eigenvector. By construction, we have $\exists!(i, j), \Lambda_k = \lambda_i \lambda'_j$ and $\mathbf{V}_k = \mathbf{v}_i \otimes \mathbf{v}'_j$. We index the eigenvalues in decreasing order of modulus, and if two are of equal modulus, we index them based on λ_i .

2.4 Differential Characteristic Function

An attractor is obtained by recursively applying the operators of a P-IFS to a set of compacts. If we focus on a single operator T , we get a sequence of points that starts from a point q of \mathbb{B}^N and converges towards the fixed point of the operator as we iteratively apply T .

The Differential Characteristic Function (DCF), defined by Janbein et al. (Janbein et al., 2024), is a

parametric function that interpolates the sequence of points obtained by recursively applying T to a starting point q . It was introduced to capture the differential properties of this sequence of points, as illustrated in Figure 2. For any operator T and starting point q , the DCF is defined as:

$$DCF(T, q, t) = \sum_{i=0}^{N-1} x_i \mathbf{v}_i t^{\alpha_i} \quad (1)$$

where the x_i are the coordinates of q in the eigenbasis of T and $\alpha_i = \frac{\log(|\lambda_i|)}{\log(|\lambda_1|)}$.

This parametric representation is used as a way to compute the curvature of a fractal curve at an extremity (the fixed point of the operator T). Due to the fractal nature of the attractor, there is not only one single DCF, but a family of DCF when all the points of the attractor are considered as starting points. The key point of this approach is that we can infer a range of curvatures from this family of DCF (Janbein et al., 2024). There are three cases depending on the value of α_2 in Equation 1:

- if $\alpha_2 < 2$, the curvatures of the range are infinite at the fixed point, no matter their starting point,
- if $\alpha_2 = 2$, the curvatures of the range are finite and non-null, no matter their starting point, at the fixed point,
- if $\alpha_2 > 2$, the curvatures of the range vanish at the fixed point, no matter their starting point.

These cases are illustrated in Figure 3.

For differentiable curves such as Bezier curves, where only a single DCF is superimposed with the attractor, we obtain only a single value for the pseudo-curvature that corresponds to the curvature.

Any point of a given DCF D_1 taken as a new starting point will generate a new DCF D_2 that is superimposed with D_1 , but with a different parametrisation.

Property 2.1. *The graph of the DCF of any contractive operator T is invariant under the DCF*

Proof. Let $\dot{q} = DCF(T, q, r) = \sum_{i=0}^{N-1} x_i \mathbf{v}_i r^{\alpha_i}$. The coordinates of \dot{q} in the eigenbasis of T are: $\dot{x}_i = x_i r^{\alpha_i}$. If we take the DCF of T from \dot{q} we have: $DCF(T, \dot{q}, t) = \sum_{i=0}^{N-1} \dot{x}_i r^{\alpha_i} \mathbf{v}_i t^{\alpha_i} = \sum_{i=0}^{N-1} x_i \mathbf{v}_i (rt)^{\alpha_i} = DCF(T, q, rt)$. \square

We can apply the DCF on an operator $\mathcal{T} = T \otimes T'$ exactly as it was defined for non-tensor product P-IFS.

$$DCF(\mathcal{T}, Q, t) = \sum_{i=0}^{NM-1} X_i \mathbf{V}_i t^{\Lambda_i}$$

$$DCF(\mathcal{T}, Q, t) = \sum_{i=0}^{N-1} \sum_{j=0}^{M-1} x_i x'_j \mathbf{v}_i \otimes \mathbf{v}'_j t^{\alpha_i \alpha'_j}$$

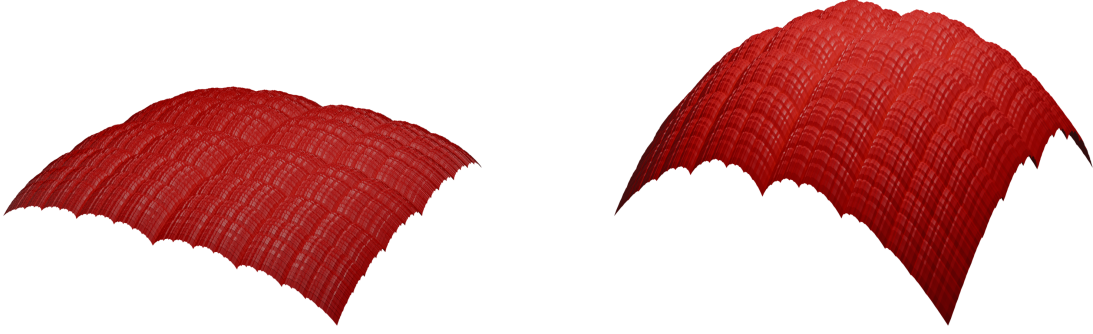


Figure 1: The attractors of two P-IFS that are the tensor product of two Takagi-like IFS. The operators of the IFS share their second eigenvectors, but their tangent plane (defined by their first eigenvectors) changes, resulting in a similar geometry, but a varied height amplitude.

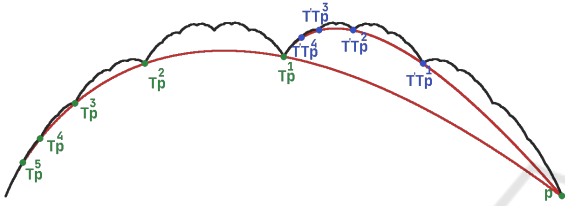


Figure 2: A P-IFS composed of two operators (T and T'), whose attractor (in black) is the Takagi curve. Two DCF in red illustrated how the point p is transformed when applying T^n (in green) and $T'T^n$ (in blue). Note that the DCF with the blue points is exactly the DCF with the green points transformed by T' .

where X_i is the coordinates of Q in the eigen basis $(\mathbf{V}_0, \mathbf{V}_1, \dots, \mathbf{V}_{NM-1})$ and $A_i = \frac{\log(|\Lambda_i|)}{\log(|\Lambda_1|)}$. Note that $A_0 = 0$ (thus $t^{A_0} = 1$) and $A_1 = 1$; When an eigenvalue is negative, a point q will jump to a different half-plane split by the eigenvectors. This is described in more details in section 4.

3 SURFACE DCF

Our objective is to provide a tool to analyse the curvatures of a fractal surface generated from the tensor product of fractal curves.

Considering the results obtained on DCF (detailed in the previous part) for a fractal surface would be like analysing a directional derivative of the surface (at the fixed point), which is insufficient. Moreover, analysing all DCF that are in all directions would be too complex and chaotic. Hence we need a parametric representation that captures the limit behavior of the surface locally at each fixed point.

We propose to construct a Surface Differential Characteristic Function (SDCF) of an operator $\mathcal{T} = T \otimes T'$ as the tensor product of the DCF of T and T' . We claim that it captures the differential properties of the attractor at the fixed point of \mathcal{T} and is infinitely

differentiable.

The SDCF is a bivariate function defined by :

$$\text{SDCF}(\mathcal{T}, Q, s, t) = \text{DCF}(T, q, s) \otimes \text{DCF}(T', q', t)$$

From the definition of the DCF (Janbein et al., 2024), we obtain:

$$\text{SDCF}(\mathcal{T}, Q, s, t) = \sum_{i=0}^{N-1} \sum_{j=0}^{N'-1} x_i x'_j \mathbf{v}_i \otimes \mathbf{v}'_j s^{\alpha_i} t^{\alpha'_j}$$

An illustration of a SDCF is shown in Figure 4.

We introduce the notation $\mathbf{D}_{i,j} = x_i x'_j \mathbf{v}_i \otimes \mathbf{v}'_j$, which corresponds to the variable-independent part of the SDCF formula.

As for DCF, any point of a given SDCF SD_1 taken as a new starting point will generate a new SDCF SD_2 that is superimposed with SD_1 , but with a different parametrisation.

Property 3.1. *The graph of the SDCF of an operator \mathcal{T} is invariant under the SDCF.*

Proof. Let $\dot{q} = \text{SDCF}(\mathcal{T}, q, u, r) = \sum_{i=0}^{N-1} \sum_{j=0}^{N'-1} \mathbf{D}_{i,j} u^{\alpha_i} r^{\alpha'_j}$. Given the coordinates of \dot{q} in the eigenbasis: $\dot{x}_i = x_i x'_j u^{\alpha_i} r^{\alpha'_j}$. If we take the SDCF of \mathcal{T} from \dot{q} we have: $\text{SDCF}(\mathcal{T}, \dot{q}, s, t) = \sum_{i=0}^{N-1} \sum_{j=0}^{N'-1} \dot{x}_i \dot{x}'_j \mathbf{v}_i \otimes \mathbf{v}'_j s^{\alpha_i} t^{\alpha'_j} = \sum_{i=0}^{N-1} \sum_{j=0}^{N'-1} x_i x'_j u^{\alpha_i} r^{\alpha'_j} \mathbf{v}_i \otimes \mathbf{v}'_j s^{\alpha_i} t^{\alpha'_j} = \sum_{i=0}^{N-1} \sum_{j=0}^{N'-1} \mathbf{D}_{i,j}(us)^{\alpha_i} (rt)^{\alpha'_j} = \text{SDCF}(\mathcal{T}, q, us, rt)$. \square

The following property justifies the definition of SDCF. It states that the DCF defined from an operator of the P-IFS of the surface ($\mathcal{T} = T \otimes T'$) is included in the tensor product of the two DCF defined from T and T' .

Property 3.2. *The DCF of T from any point q in \mathbb{B}^N is an embedding of the DCF of \mathcal{T} from $q \otimes \mathbf{v}'_0$, i.e. $\text{DCF}(T, q, t) \otimes \mathbf{v}'_0 = \text{DCF}(\mathcal{T}, q \otimes \mathbf{v}'_0, t)$.*



Figure 3: Three P-IFS (having two operators) with $\alpha_2 = 1.5$ on the left, $\alpha_2 = 2$ in the middle, and $\alpha_2 = 2.5$ on the right. Here only λ_2 and ν_2 were changed for the left operator.

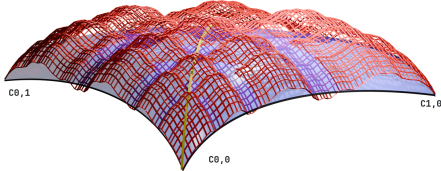


Figure 4: The attractor of a P-IFS that is the tensor product of two P-IFS $\mathbb{T} = \{T_0, T_1\}$ and $\mathbb{T}' = \{T'_0, T'_1\}$ is represented in wireframe (red). The DCF of T_0 and T'_0 (having respectively $C_{1,0}$ and $C_{0,1}$ as starting points) are in black. The DCF of $T_{0,0} = T_0 \otimes T'_0$ having $C_{1,1}$ as starting point is represented in yellow. Finally, the SDCF of $T_{0,0}$ having $C_{1,1}$ as starting point is represented in light blue. Note that all 3 DCF are included in the SDCF.

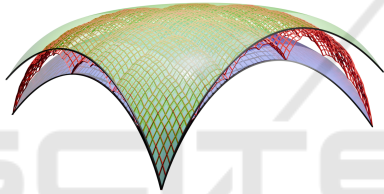


Figure 5: A P-IFS whose attractor (in red wireframe) is the tensor product of two Takagi curves. The minimum and maximum SDCF are shown in light blue and green respectively.

Proof. We take q a point of \mathbb{B}^N . $q \otimes v'_0$ refers to q embedded in \mathbb{B}^{NM} according to v'_0 .

$$DCF(\mathcal{T}, q \otimes v'_0, t) = \sum_{i=0}^{N-1} \sum_{j=0}^{N'-1} x_i x'_j \mathbf{v}_i \otimes \mathbf{v}'_j t^{\alpha_i \alpha'_j}.$$

x'_j is 0 except for $x'_0 = 1$. Thus, we have $DCF(\mathcal{T}, q \otimes v'_0, t) = \sum_{i=0}^{N-1} x_i \mathbf{v}_i \otimes \mathbf{e}_{N',0} t^{\alpha_i} \equiv \sum_{i=0}^{N-1} x_i \mathbf{v}_i t^{\alpha_i} = DCF(\mathcal{T}, q, t)$. \square

The previous property is also true for $v_0 \otimes q'$.

Another strong property is that the DCF with a starting point on a SDCF is included in the SDCF.

Property 3.3. *The SDCF of \mathcal{T} from any point q contains the DCF of \mathcal{T} from q .*

Proof. $SDCF(\mathcal{T}, q, t, t) = \sum_{i=0}^{N-1} \sum_{j=0}^{N'-1} \mathbf{D}_{i,j} t^{\alpha_i \alpha'_j} = \sum_{i=0}^{N-1} \sum_{j=0}^{N'-1} \mathbf{D}_{i,j} t^{\alpha_i + \alpha'_j} = DCF(\mathcal{T}, q, t)$ \square

4 TANGENT AT THE FIXED POINT OF AN OPERATOR

Given a contractive operator T with strictly decreasing eigenvalues, the eigenvector (ν_1) associated with the second greatest eigenvalue is the pseudo-tangent at the fixed point (Bensoudane, 2009). However, there are special cases to consider:

- $\lambda_1 < 0$: the point q will jump from one half-plane delimited by ν_2 to the other, resulting in a range of tangents that spans the sector delimited by ν_1 to $-\nu_1$.
- $\lambda_2 < 0$: the point q will jump from one half-plane delimited by ν_1 to the other, while still converging along ν_1 , see Figure 7.

Note that there might be a transformation with both $\lambda_1 < 0$ and $\lambda_2 < 0$, but the attractor of an IFS with such a transformation would be ill-suited to generate surfaces, so this case is ignored.

Figures 5 and 6 illustrate some situations that arise for surfaces. Figure 5 showcases a minimum and maximum SDCF while Figure 6 presents some remarkable combination of DCF.

The pseudo-tangents at the fixed point are the same as the pseudo-tangents defined by Bensoudane et al. (Bensoudane, 2009) and Podkorytov et al. (Podkorytov, 2013).

In the case of SDCF, we have pseudo-tangent-plane at the fixed point that contains the pseudo-tangents of the two DCF and delimits half-spaces. If some eigenvalues of T and T' are negative, the point Q will jump from one half-space to the other.

5 CURVATURE AT FIXED POINTS

Thanks to the SDCF, which is an analytically defined surface, we can calculate curvatures which can then be used to estimate pseudo-curvatures of the fractal surface and characterise its differential behaviour at fixed points.

For a surface $\mathcal{F}(s, t)$, the curvatures are computed from the first and second fundamental forms (noted I and II below):

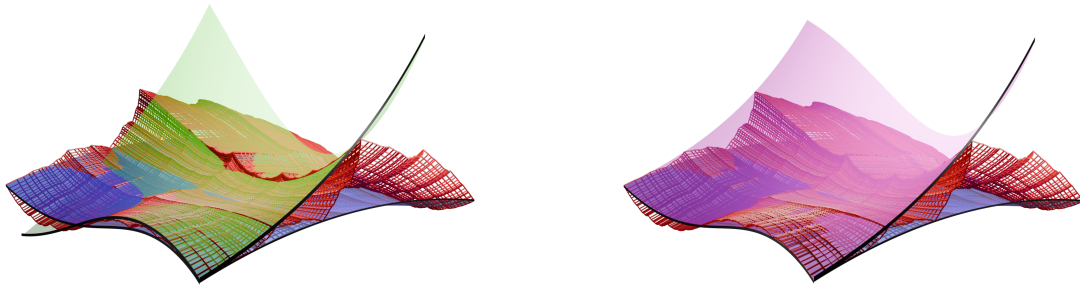


Figure 6: A P-IFS whose attractor (in red wireframe) is the tensor product of a Takagi curve and the curve in figure 7 (with a negative λ_2). The SDCF in blue is the tensor product of the minimum DCF of the Takagi curve and the DCF that capture the behavior of $T^n q$ for even n . The SDCF in green is the tensor product of the maximum DCF of the Takagi curve and the DCF that capture the behavior of $T^n q$ for odd n . The SDCF in pink is the tensor product of the minimum DCF of the Takagi curve and the DCF that captures the behavior of $T^n q$ for odd n .

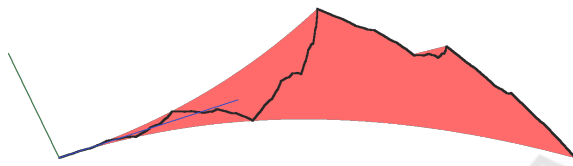


Figure 7: A P-IFS with λ_2 negative. Applying T_0 to a point makes it jump from one side of \mathbf{v}_1 (in blue) to the other.

$$I = \begin{pmatrix} E & F \\ F & G \end{pmatrix}, II = \begin{pmatrix} L & M \\ M & N \end{pmatrix}$$

$$E = \frac{\partial \mathcal{F}(s,t)^2}{\partial s}; G = \frac{\partial \mathcal{F}(s,t)^2}{\partial t}$$

$$F = \frac{\partial \mathcal{F}(s,t)}{\partial s} \cdot \frac{\partial \mathcal{F}(s,t)}{\partial t}$$

$$L = \frac{\partial^2 \mathcal{F}(s,t)}{\partial s^2} \cdot \mathbf{n}_{s,t}; N = \frac{\partial^2 \mathcal{F}(s,t)}{\partial t^2} \cdot \mathbf{n}_{s,t}$$

$$M = \frac{\partial^2 \mathcal{F}(s,t)}{\partial s \partial t} \cdot \mathbf{n}_{s,t}$$

with $\mathbf{n}_{s,t}$ the normal of the surface at (s,t) .

For a given parametric curve $f(t)$, we can associate to each value of t a measure of the curvature: $\kappa(t) = \frac{1}{\mathcal{R}(t)}$, where $\mathcal{R}(t)$ is the radius of curvature at t . For surfaces, we have the Gaussian curvature \mathcal{K} , the mean curvature \mathcal{H} and the two principal curvatures \mathcal{K}_1 and \mathcal{K}_2 . The Gaussian curvature $\mathcal{K}(s,t)$ describes the local shape of the surface at (s,t) .

- $\mathcal{K} < 0$, the surface is said to have an hyperbolic point at (s,t) and is saddle-shaped.
- $\mathcal{K} = 0$, the surface is flat at (s,t) in at least a direction (cylinder-like or a plane).
- $\mathcal{K} > 0$, the surface is said to have an elliptic point at (s,t) and is dome/bowl shaped.

As the SDCF approximates the fractal surface at the fixed point, we can have an idea of the differential behaviour of the surface by computing the curvatures of the SDCF. The considered fixed point is the one with $s = 0$ and $t = 0$, so it is necessary to study the limit of the curvature of the SDCF when (s,t) goes to $(0,0)$. \mathcal{K} is defined using the first and second fundamental forms as:

$$\mathcal{K} = \frac{LN - M^2}{EG - F^2}$$

Since the attractor is built as an iterative process of transformations, if we know a property at the fixed point, we can compute it on any dyadic point of the attractor. That's why we first study and compute the curvature at the fixed point: we compute the limit of the curvature as we approach the fixed point. We abbreviate $\text{SDCF}(\mathcal{T}, Q, s, t)$ as $\mathcal{F}(s, t)$.

$$\lim_{(s,t) \rightarrow (0,0)} \mathbf{n}_{s,t} = \mathbf{n}_{0,0} = \frac{PD_{1,0} \times PD_{0,1}}{\|PD_{1,0} \times PD_{0,1}\|}$$

$$\lim_{(s,t) \rightarrow (0,0)} \frac{\partial \mathcal{F}(s,t)}{\partial s} = \mathbf{D}_{1,0}; \lim_{(s,t) \rightarrow (0,0)} \frac{\partial \mathcal{F}(s,t)}{\partial t} = \mathbf{D}_{0,1}$$

$$\lim_{(s,t) \rightarrow (0,0)} \frac{\partial \mathcal{F}(s,t)}{\partial s \partial t} = \mathbf{D}_{1,1}$$

$$\lim_{(s,t) \rightarrow (0,0)} \frac{\partial^2 \mathcal{F}(s,t)}{\partial s^2} = \lim_{s \rightarrow 0} \alpha_2 (\alpha_2 - 1) \mathbf{D}_{2,0} s^{\alpha_2 - 2}$$

$$\lim_{(s,t) \rightarrow (0,0)} \frac{\partial^2 \mathcal{F}(s,t)}{\partial t^2} = \lim_{t \rightarrow 0} \alpha'_2 (\alpha'_2 - 1) \mathbf{D}_{0,2} t^{\alpha'_2 - 2}$$

We introduce the following notations:

$$\mathcal{K}_s(s) = P \alpha_2 (\alpha_2 - 1) \mathbf{D}_{2,0} s^{\alpha_2 - 2}$$

$\mathcal{K}_t(t) = P \alpha'_2 (\alpha'_2 - 1) \mathbf{D}_{0,2} t^{\alpha'_2 - 2}$ The computation of the limit of the Gaussian curvature of the SDCF at

the point $(0, 0)$ is expressed as follows:

$$\lim_{(s,t) \rightarrow (0,0)} \frac{\mathcal{K}_G(s) \cdot \mathbf{n}_{s,t} \mathcal{K}_L(t) \cdot \mathbf{n}_{s,t} - (PD_{1,1} \cdot \mathbf{n}_{s,t})^2}{(PD_{1,0})^2 \cdot (PD_{0,1})^2 - (PD_{1,0} \cdot PD_{0,1})^2}$$

Note that the denominator is a constant: $(PD_{1,0})^2(PD_{0,1})^2 - (PD_{1,0} \cdot PD_{0,1})^2$. This constant equals 0 if $(PD_{1,0})^2 \cdot (PD_{0,1})^2 = (PD_{1,0} \cdot PD_{0,1})^2$. From the Cauchy-Schwarz inequality, we know that this equality holds only if $PD_{0,1}$ and $PD_{1,0}$ are linearly dependent.

We have 3 cases for the Gaussian curvature of each operator:

- $\alpha_2 < 2$: the first term $\alpha_2(\alpha_2 - 1)D_{2,0}s^{\alpha_2-2} \cdot \mathbf{n}_{0,0}$ is infinite and all other terms don't matter ($\lim_{s \rightarrow 0} s^{\alpha_i-2} = \infty$)
- $\alpha_2 = 2$: the first term $\alpha_2(\alpha_2 - 1)D_{2,0}s^{\alpha_2-2}$ is a constant and all other terms are either constant or null.
- $\alpha_2 > 2$ all terms vanish ($\alpha_i - 2$ will always be positive so $\lim_{s \rightarrow 0} s^{\alpha_i-2} = 0$)

Assuming we do not have the degenerate case with linearly dependent vectors, we have 9 possibilities when we combine the cases of \mathcal{K}_G and \mathcal{K}_L for the Gaussian curvature:

- $\alpha_2 > 2, \alpha'_2 > 2$: the limit of \mathcal{K}_G and \mathcal{K}_L is infinite, so the curvature is infinite,
- $\alpha_2 > 2, \alpha'_2 = 2$: the limit of \mathcal{K}_G is infinite and the limit of \mathcal{K}_L is finite and non-null, so the curvature is infinite,
- $\alpha_2 > 2, \alpha'_2 < 2$: the limit of \mathcal{K}_G is infinite and the limit of \mathcal{K}_L is null, so the curvature does not exist,
- $\alpha_2 = 2, \alpha'_2 = 2$: the limit of \mathcal{K}_G and \mathcal{K}_L is finite and non-null, so the curvature is finite and is $\frac{PD_{2,0} \cdot \mathbf{n}_{0,0} PD_{0,2} \cdot \mathbf{n}_{0,0} - (PD_{1,1} \cdot \mathbf{n}_{s,t})^2}{(PD_{1,0})^2 \cdot (PD_{0,1})^2 - (PD_{1,0} \cdot PD_{0,1})^2}$,
- $\alpha_2 = 2, \alpha'_2 < 2$: the limit of \mathcal{K}_G is finite and non-null \mathcal{K}_L null, so the curvature is finite and is $\frac{-(PD_{1,1} \cdot \mathbf{n}_{s,t})^2}{(PD_{1,0})^2 \cdot (PD_{0,1})^2 - (PD_{1,0} \cdot PD_{0,1})^2}$
- $\alpha_2 < 2, \alpha'_2 < 2$: the limit of \mathcal{K}_G and \mathcal{K}_L is null, so the curvature is finite and is $\frac{-(PD_{1,1} \cdot \mathbf{n}_{s,t})^2}{(PD_{1,0})^2 \cdot (PD_{0,1})^2 - (PD_{1,0} \cdot PD_{0,1})^2}$.

We summarize the preceding cases in the following table:

$\lim_{(s,t) \rightarrow (0,0)} \mathcal{K}$	$\alpha_2 < 2$	$\alpha_2 = 2$	$\alpha_2 > 2$
$\alpha'_2 < 2$	$\pm\infty$	$\pm\infty$	\emptyset
$\alpha'_2 = 2$	$\pm\infty$	\mathcal{K}	\mathcal{K}
$\alpha'_2 > 2$	\emptyset	\mathcal{K}	\mathcal{K}

For the mean and principal curvatures, the calculations are carried out in the same way.

6 CURVATURE OF AN ATTRACTOR

The computation of the curvature on a differentiable curve gives a unique value at each point of the curve. For nowhere differentiable curves like fractals, Janbein et al. (Janbein et al., 2024) have computed pseudo-curvatures (in the form of curvature ranges) at each side of every dyadic points. For surfaces, where multiple curvature metrics exist (Gaussian, Mean and principal curvatures), we find again a range for each of these values. Depending on the starting point, the SDCF changes, resulting in a family of SDCF whose volume acts as a hull to the attractor. As for nowhere differentiable curves, where pseudo-curvatures are first computed (in the form of curvature ranges) at the fixed point of each operator T and then deduced at each side of every dyadic points, the same apply for tensor product fractal surfaces. It hence gives us the opportunity to characterize the nature of a tensor product fractal surface (defined by four operators) at any dyadic point, that can be: concave/convex ellipsoid, cylindrical, hyperboloid ...

7 CONCLUSION

In this paper, we have extended the definition of the pseudo-curvature from P-IFS-generated curves to tensor product fractal surfaces. This was done through the definition of the SDCF, seen as the tensor product of the two DCF associated to the curves from which the attractor is formed.

Taking the first derivative of a SDCF results in a pseudo-tangent that accurately represent the first order differential behavior of the attractor. The second derivative of a SDCF yields pseudo-curvatures that correspond to the second order differential behavior of the surface. Unlike for smooth surfaces that have a single value of curvature per point, we have shown that fractal surfaces have ranges of pseudo-curvatures, due to the intricate complexity of their geometry. The pseudo-curvature computation is based on the analysis of their eigenvalues and eigenvectors (for each implied operator). As a future work, we would like to explore how the control of the second order differential behavior of the surface (via the eigen values and vectors) can have an influence on its perceived roughness. It hence would give us the opportunity to control roughness, as shown in Figure 8.

We are also interested in studying the DCF (resp. SDCF) of P-IFS with more than two (resp. four) transformations. This study must take particular attention to the fixed points of the non-extrema transfor-

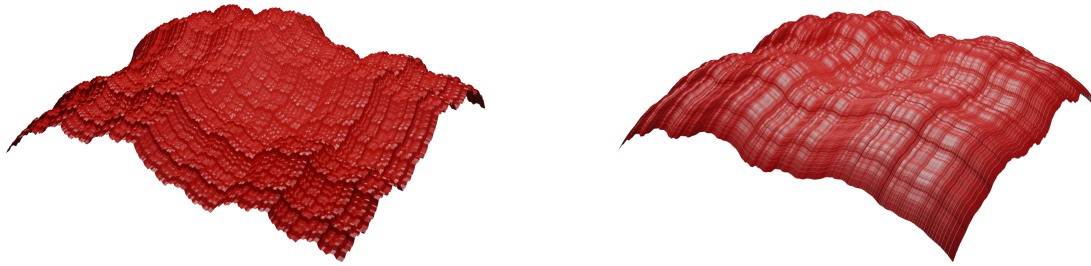


Figure 8: The attractors of two P-IFS with a similar geometry, but with widely different range of pseudo-curvature, resulting in a different roughness.

mations. Ensuring continuity at every junction points is not enough to guarantee continuity at every dyadic point on such curves and surfaces. Then, we are interested in the differential properties of fractals that can be constructed using Controlled Iterated Function System C-IFS that extends the definition of the plain IFS or P-IFS with an automaton that decides which operator to apply, based on the current state and its transition rules, allowing a larger variety of possible surfaces. Finally we would like to generalize our results to non tensor-product fractal surfaces, which is more complex than the case of tensor product surface, both because of the freer transformations, and the potentially non-grid subdivision scheme.

ACKNOWLEDGEMENTS

This work benefited from the support of the project Fraclettes ANR-20-CE46-0003 of the French National Research Agency (ANR).

REFERENCES

- Banach, S. (1922). Sur les opérations dans les ensembles abstraits et leur application aux équations intégrales. *Fundamenta Mathematicae*, 3:133–181.
- Barnsley, M. F. (1986). Fractal functions and interpolation. *Constructive Approximation*, 2(1):303–329.
- Barnsley, M. F. (1988). *Fractals Everywhere*. Dover Publications, Inc.
- Bensoudane, H. (2009). *Etude différentielle des formes fractales*. PhD thesis, Université de Bourgogne.
- Bensoudane, H., Gentil, C., and Neveu, M. (2009). Fractional half-tangent of a curve described by iterated function systems. *Journal Of Applied Functional Analysis*, 4(2).
- Bigerelle, M., Nianga, J.-M., Najjar, D., Iost, A., Hubert, C., and Kubiak, K. (2013). Roughness signature of tribological contact calculated by a new method of peaks curvature radius estimation on fractal surfaces. *Tribology International*, 65:235–247.
- Bolzano, B. (1950). *Paradoxes of the Infinite*. Rare masterpieces of philosophy and science. Routledge and Paul.
- Hutchinson, J. E. (1981). Fractals and self similarity. *Indiana University Mathematics Journal*, 30:713–747.
- Janbein, M., Gentil, C., Roudet, C., and Poull, C. (2024). Pseudo-curvature of fractal curves for geometric control of roughness. In *19th International Conference on Computer Graphics Theory and Applications*, volume 1 of *GRAPP, HUCAPP and IVAPP*, pages 177–188, Rome, Italy.
- Lindenmayer, A. (1968). Mathematical models for cellular interactions in development ii. simple and branching filaments with two-sided inputs. *Journal of Theoretical Biology*, 18(3):300–315.
- Podkorytov, S. (2013). *Espaces tangents pour les formes auto-similaires*. PhD thesis, Université de Bourgogne.
- Podkorytov, S., Gentil, C., Sokolov, D., and Lanquetin, S. (2013). Geometry control of the junction between two fractal curves. *Computer-Aided Design*, 45(2):424–431.
- Podkorytov, S., Gentil, C., Sokolov, D., and Lanquetin, S. (2014). Joining primal/dual subdivision surfaces. In *Mathematical Methods for Curves and Surfaces: 8th International Conference, MMCS 2012, Oslo, Norway, June 28–July 3, 2012, Revised Selected Papers 8*, pages 403–424. Springer.
- Takagi, T. (1901). A simple example of the continuous function without derivative. *Tokyo Sugaku-Butsurigakkwai Hokoku*, 1:F176–F177.
- Zair, C. E. (1998). *Formes fractales à pôles basées sur une généralisation des IFS*. PhD thesis, Université Claude Bernard-LYON-1.
- Zair, C. E. and Tosan, E. (1996). Fractal modeling using free form techniques. In *Computer Graphics Forum*, volume 15, pages 269–278. Wiley Online Library.